Stimulator of interferon genes signaling network-driven prognostic signature for pancreatic cancer: Hub gene discovery with multimodal validation

WENJING YU[1*], JUNQUN LIAO[2*], JIAYAN LI[3] and YONGQUAN WU[3]

[1]The Medical Laboratory of Science, The Thirteenth People's Hospital of Chongqing, Chongqing 400084, P.R. China;
[2]The Medical Laboratory of Science, The First Affiliated Hospital of Chongqing Medical University, Chongqing 400084, P.R. China;
[3]Zhongyuan Huiji Biotechnology Co., Ltd. (Zybio Inc.), Chongqing 400084, P.R. China

Received February 23, 2025; Accepted August 6, 2025

DOI: 10.3892/ol.2025.15348

Abstract. The stimulator of interferon genes (STING) signaling pathway plays an important role in tumor progression, particularly in immune regulation. However, the functions of STING-related genes in immunologically 'cold' tumors, such as pancreatic ductal adenocarcinoma (PAAD), are yet to be elucidated. The present study aims to investigate the involvement of STING signaling pathway-associated genes in PAAD progression and immune infiltration. Bioinformatics analysis of PAAD transcriptomic data from public cohorts (TCGA and GEO) revealed that the majority of STING-related genes were highly expressed in PAAD. Based on the expression levels of these genes, patients with PAAD from these cohorts were stratified into high-risk and low-risk groups. These STING-related genes exerted differential impacts on tumor mutational burden, immune infiltration and response to immunotherapy. Utilizing these genes, a prognostic model was constructed (hazard ratio, 2.639; P<0.001) and externally validated. Model analysis indicated that interferon-induced protein with tetratricopeptide repeats 2 (IFIT2) and zinc finger DHHC-type containing 1 (ZDHHC1) may possess notable biological functions in PAAD. Subsequent functional experiments involving knockout of IFIT2 and overexpression of ZDHHC1in PAAD cell lines demonstrated that these genes significantly regulated cell proliferation (assessed by CCK-8 assay) and apoptosis (assessed by TUNEL assay) (P<0.001). In summary, the STING signaling pathway is critically involved in PAAD pathogenesis, and the representative genes IFIT2 and ZDHHC1 exhibit distinct functional roles within this context.

Correspondence to: Dr Yongquan Wu, Zhongyuan Huiji Biotechnology Co., Ltd. (Zybio Inc.), Building 4, 104 CuiBai Road, Dadukou, Chongqing 400084, P.R. China
E-mail: 13883914746@163.com

*Contributed equally

Abbreviations: PAAD, pancreatic ductal adenocarcinoma; STING, stimulator of interferon genes; IFIT2, interferon-induced protein with tetratricopeptide repeats 2; ZDHHC1, zinc finger DHHC-type containing 1; LASSO, least absolute shrinkage and selection operator; TME, tumor microenvironment; TIDE, Tumor Immune Dysfunction and Exclusion; CCK-8, Cell Counting Kit-8; TCGA, The Cancer Genome Atlas

Key words: STING, immune filtration, prognostic, pancreatic cancer

Introduction

Globally, pancreatic ductal adenocarcinoma (PAAD) accounted for 511,000 new cases and 467,000 deaths in 2022 (according to GLOBOCAN data), ranking as the sixth leading cause of cancer-related mortality worldwide at present and contributing to 5% of all cancer-associated deaths. This mortality rate places PAAD among the malignancies with the poorest prognosis (1). PAAD, while exhibiting a relatively low incidence rate, carries a disproportionately high mortality rate. Global epidemiological data indicate a rising incidence of PAAD annually (2). Although less prevalent than a number of other malignancies, PAAD imparts a worse prognosis due to challenges in early detection and effective treatment (3). Established risk factors for PAAD development include smoking, obesity, high-fat diets, chronic pancreatitis and genetic predisposition. Smoking constitutes a primary modifiable risk factor, while genetic and environmental influences also contribute markedly to disease susceptibility (4). Current therapeutic modalities for PAAD are primarily limited to surgical resection, supplemented by radiotherapy, chemotherapy or targeted agents such as Erlotinib (5). However, clinical outcomes often remain suboptimal. Immunotherapy has emerged as a promising therapeutic paradigm, aiming to harness the host immune system to eradicate cancer cells (6). Consequently, immune checkpoint inhibitors and related immunotherapeutics are being evaluated in subsets of patients with PAAD (7). However, the inherent immunological 'cold' nature of PAAD presents a major barrier to immunotherapy efficacy. Converting these immunologically quiescent tumors into 'hot', immune-responsive lesions represents an important requirement for immunotherapy efficacy (8).

The stimulator of interferon genes (STING) pathway represents a pivotal innate immune modulator with the potential to convert immunologically 'cold' tumors into 'hot' microenvironments (9). STING activation triggers the production of type I interferons (IFNs) and other cytokines, thereby reshaping the tumor microenvironment (TME) and modulating immune cell activity (10). While STING pathway activation has been linked to tumor progression and metastasis in certain contexts, often regulated by epigenetic mechanisms such as DNA methylation (11), its therapeutic manipulation holds promise. At present, STING agonists are undergoing clinical trials to evaluate their efficacy in patients with advanced cancer. Furthermore, the potential application of STING agonists in early-stage disease (12), particularly before the establishment of robust immune evasion mechanisms within the TME, is an active area of investigation (13). Within the specific context of PAAD, preclinical studies suggest that STING activation can stimulate type I IFN production and promote dendritic cell (DC) maturation (14). Despite this promise, successful clinical translation faces notable hurdles, including: i) An incomplete understanding of PAAD-specific STING interactome dynamics (15); ii) the induction of compensatory immunosuppressive mechanisms (e.g., myeloid-derived suppressor cell expansion) that counteract agonist efficacy (16); and notably, iii) the absence of validated predictive biomarkers to stratify patients likely to respond to STING activation treatment (17). Moreover, the efficacy of STING agonists in PAAD may be contingent upon the specific TME composition, patient genetics and the specific combination partners used (e.g., chemotherapy or immune checkpoint inhibitors), as synergistic interactions can significantly enhance their therapeutic effect (18,19). In conclusion, elucidating the mechanistic role and therapeutic potential of the STING pathway in cancer immunotherapy has become a major research focus. Such investigations are important not only for deepening the present understanding of PAAD pathogenesis but also for developing novel and effective therapeutic strategies against recalcitrant PAAD malignancy.

The present study aimed to systematically map the core regulatory components within the STING signaling-protein interactome to construct a prognostic signature for PAAD. Interactome mapping was pursued through comprehensive protein-protein interaction network-centrality analysis. Collectively, by decoding the STING-centered protein network, the present study seeks to identify novel tractable targets for potentiating STING agonism in PAAD treatment.

Material and methods

Bioinformatics

Patient data. Samples from a total of 353 patients with pancreatic cancer were integrated from The Cancer Genome Atlas (TCGA)-pancreatic adenocarcinoma (n=178) and GSE224564 (n=175) datasets, and cases with incomplete clinical data were excluded. The RNA sequencing and clinical data of 178 patients with PAAD were obtained from TCGA (https://www.cancer.gov/). The PAAD dataset GSE224564 (20) was downloaded from GEO (www.ncbi.nlm.nih.gov/geo/query/acc.cgi) and included the RNA sequencing and clinical data of 175 patients with PAAD.

Bioinformatic analysis. Differential gene expression between STING-based subtypes (C1 vs. C2) was analyzed using DESeq2 (v1.38.3). Functional enrichment was performed via clusterProfiler (v4.0) using annotations from the Gene Ontology Consortium (http://geneontology.org) and KEGG Pathway Database (https://www.genome.jp/kegg/), with significance defined as a Benjamini-Hochberg adjusted P-value <0.05. TME scores (immune/stromal) and tumor purity were calculated using the ESTIMATE algorithm (v1.0.13; https://bioinformatics.mdanderson.org/estimate/). Immune cell infiltration was deconvoluted with CIBERSORTx (https://cibersortx.stanford.edu) using the LM22 signature matrix and 1,000 permutations. Mutation profiles were processed via Maftools (v2.16.0) with TCGA somatic mutation data. All statistical thresholds are explicitly stated in figure legends. Gene Ontology (GO) and Kyoto Encyclopedia of Genes and Genomes (KEGG) pathway enrichment analyses were performed to interpret the functional significance of the identified genes. GO analysis (http://geneontology.org) was utilized to categorize genes into biological processes, molecular functions and cellular components. KEGG pathway analysis (https://www.genome.jp/kegg/) was used to identify significantly enriched signaling and metabolic pathways. The analyses were performed using the clusterProfiler R package (v4.0), with a significance threshold of an adjusted P-value <0.05.

Construction of STING pathway-related gene prognostic signature in PAAD. Curated Cancer Cell Atlas (www.weizmann.ac.il/sites/3CA/) was used to identify the expression of STING in the TME. STRING (cn.string-db.org) and Genemiania (genemania.org) were used to identify 26 STING pathway-related genes (Table SI). The association between STING pathway-related genes and the prognosis of patients with PAAD was evaluated via univariate cox regression. A least absolute shrinkage and selection operator (LASSO) Cox regression analysis was used for constructing the signature for STING pathway-related genes. Bioinformatics analysis of PAAD transcriptomic data from public cohorts (TCGA and GEO) revealed that the majority of STING-related genes were highly expressed in PAAD (significance defined as |log2(fold change)|>1 and adjusted P-value <0.05). Based on the expression levels of these genes, PAAD patients from these cohorts were stratified into high-risk and low-risk groups. These STING-related genes exerted differential impacts on tumor mutational burden, immune infiltration and response to immunotherapy. Prognostic STING pathway-related genes were then selected via stepwise multivariate Cox regression using the Akaike information criterion for model optimization. Utilizing these genes, a prognostic model was constructed (hazard ratio, 2.639; P<0.001) and externally validated. Risk Score= $\sum_{k=0}^{n} coef(k) * x(k)$, where coef(k) and x(k) represented the regression coefficients. The groups were divided into high- and low-risk groups using the median risk score (1.476) as the cut-off. Univariate and multivariate Cox regression were used to evaluate independent factors, including clinical features and the risk score in PAAD. The Tumor Immune Dysfunction and Exclusion (TIDE) computational platform (https://tide.dfci.harvard.edu) was used to predict response to immunotherapy

in high- and low-risk PAAD patient groups stratified by the STING-signature risk score.

Online database. The GEPIA (http://gepia2.cancer-pku.cn/), Cbioportal (www.cbioportal.org), HPA (www.proteinatlas.org) and TISIDB (cis.hku.hk/TISIDB/index.php) databases were used to evaluate gene expression, survival and clinical stage and grade (21) in patients with PAAD.

In vitro assays

Cell culture. 293T cells (ATCC® CRL-3216™) and murine pancreatic ductal adenocarcinoma Panc02 cells (cat. no. CRL-2553) were cultured in high-glucose DMEM medium (Corning, Inc.) supplemented with 10% fetal bovine serum (Gibco; Thermo Fisher Scientific, Inc.) and 1% penicillin/streptomycin (HyClone™; Cytiva). Cells were maintained at 37˚C in a humidified 5% CO_2 incubator (Thermo Fisher Scientific, Inc.) and routinely subcultured every 2-3 days using 0.25% trypsin-EDTA (Gibco; Thermo Fisher Scientific, Inc.). Cell density was maintained at 60-80% confluency.

Lentiviral transduction. Lentiviral vectors expressing short hairpin RNAs (shRNAs) targeting interferon-induced protein with tetratricopeptide repeats (IFIT2), or corresponding scrambled control shRNAs (sh-NC), were constructed using the pLKO.1-puro backbone (cat. no. 8453; Addgene, Inc.). The shRNA sequences (Table SII) were designed using the Broad Institute TRC portal (v2.0) and validated by BLAST (https://blast.ncbi.nlm.nih.gov/Blast.cgi) to ensure target specificity. For overexpression, full-length zinc finger DHHC-type containing 1 (ZDHHC1) complementary DNA (OriGene Technologies, Inc.) was cloned into the pCDH-CMV-MCS-EF1-Puro vector (cat. no. CD510B-1; System Biosciences, LLC). In the ZDHHC1 overexpression experiment, cells transfected with the empty vector (pCDNA3.1) served as the negative control to confirm that any observed phenotypic changes were attributable to the expression of the target gene rather than the vector itself. All constructs were verified by Sanger sequencing. Lentiviral particles were produced using a second-generation system by co-transfecting 293T cells [American Type Culture Collection (ATCC)] cultured at 37˚C with the transfer vector (shRNA or overexpression plasmid), packaging plasmid psPAX2 (cat. no. 12260; Addgene, Inc.) and envelope plasmid pMD2.G (cat. no. 12259; Addgene, Inc.) at a 4:3:1 ratio (6:4.5:1.5 μg) using Lipofectamine® 3000 (cat. no. L3000015; Thermo Fisher Scientific, Inc.). Following a 48- to 72-h transfection period, viral supernatants were harvested, filtered through 0.45-μm PVDF membranes, and concentrated by ultracentrifugation (25,000 x g, at 4˚C for 2 h). Panc02 cells were seeded in 6-well plates ($5x10^4$ cells/well) and incubated until 40% confluency. Cells were transduced with a multiplicity of infection of 15 used to infect cells with lentivirus in the presence of 8 μg/ml polybrene (cat. no. H9268; MilliporeSigma). After 24 h, the medium was replaced with fresh complete DMEM. Transduced cells were selected using 5 μg/ml puromycin (cat. no. ant-pr-1; InvivoGen) for 72 h. Positively selected cells were then maintained in 2 μg/ml puromycin-containing medium for all subsequent experiments to ensure stable expression. Knockdown or overexpression efficacy was validated 7 days post-selection.

Western blotting. Panc02 cells (ATCC CRL-2553™) were lysed in RIPA buffer (25 mM Tris-HCl pH 7.6, 150 mM NaCl, 1% NP-40, 1% sodium deoxycholate and 0.1% SDS) supplemented with protease inhibitor cocktail (cat. no. 11836170001; Roche Diagnostics, GmbH). Protein concentration was determined by BCA assay. Samples (40 μg/lane) were denatured in Laemmli buffer at 100˚C for 10 min, separated on 10% gels using SDS-PAGE (GenScript), and transferred to PVDF membranes (cat. no. IPVH00010; MilliporeSigma). Membranes were blocked with 5% non-fat skimmed milk (cat. no. 1706404; Bio-Rad Laboratories, Inc.) in 0.1% TBST for 1 h at 25˚C, followed by overnight incubation at 4˚C with the following primary antibodies: Anti-IFIT2 (1:1,000; cat. no. ab305231; Abcam), anti-ZDHHC1 (1:1,000; cat. no. ab223042; Abcam) and anti-GAPDH (1:1,000; cat. no. CST 2118; Cell Signaling Technology, Inc.). After TBST washes, membranes were incubated with HRP-conjugated goat anti-rabbit IgG (1:100,000; cat. no. 31460; Invitrogen; Thermo Fisher Scientific, Inc.) for 1 h at 25˚C. Signals were developed using SuperSignal™ West Pico PLUS substrate (cat.no. 34577; Thermo Fisher Scientific, Inc.) and imaged with a ChemiDoc™ MP System (Bio-Rad Laboratories, Inc.) controlled by Image Lab™ Software v6.1. Band intensity was quantified by built-in densitometry tools.

Cell Counting Kit-8 (CCK-8 assay). In a standard 96-well plate, cells were seeded at 5,000 Panc02 cells per well (in 100 μl DMEM). The cells were then incubated in a 37˚C, 5% CO_2 cell culture incubator for 24 h. Having pre-calculated the corresponding seeding volume per well, CCK-8 solution (cat. no. CK04-13; Dojindo Laboratories, Inc.) was added to each well at 10% of the total volume of the medium, and the reaction proceeded in the dark for 1 h. The difference between the OD values of the treatment group and sh-NC or vehicle was calculated, then divided by the difference between the OD values of the control cells. The resulting value was multiplied by 100% to obtain the cell survival rate.

TUNEL assay. Cells were seeded onto sterile glass coverslips placed in 24-well culture plates at a density of $5x10^4$ cells per well and allowed to adhere for 24 h. After adherence, cells were washed once with phosphate-buffered saline (PBS) and fixed with 4% paraformaldehyde in PBS at room temperature for 30 min. Fixed cells were washed three times with PBS (5 min per wash). Cell membranes were permeabilized by incubation with pre-chilled PBS containing 0.1% Triton X-100 on ice for 2 min, followed by two washes with PBS. The TUNEL assay was performed using the In Situ Cell Death Detection Kit, Fluorescein (cat. no. 11684795910; Roche Diagnostics, GmbH). The TUNEL reaction mixture was prepared according to the manufacturer's protocol by combining 50 μl Enzyme Solution (terminal deoxynucleotidyl transferase) with 450 μl Label Solution (fluorescein-dUTP). This mixture was applied to cover the samples, which were then incubated at 37˚C in a humidified dark chamber for 60 min. Unbound reagents were removed by washing three times with PBS (5 min per wash). Nuclei were counterstained with 4',6-diamidino-2-phenylindole (DAPI) at 1 μg/ml in PBS for 10 min at room temperature in the dark, followed by two final washes with PBS. Samples were mounted using ProLong Gold Antifade Mountant (cat. no. P36930; Thermo Fisher Scientific, Inc.). Apoptotic cells (green fluorescence) and total nuclei (blue fluorescence) were visualized using an Olympus BX53 fluorescence microscope

(Olympus Corporation). Quantification was performed by counting TUNEL-positive cells and total DAPI-stained nuclei in ≥10 randomly selected fields of view per sample at x200 magnification.

Statistical analysis. For the statistical analysis component of this study, R software (version 4.3.2; The R Foundation for Statistical Computing) was used. This open-source software was downloaded from the Comprehensive R Archive Network (https://cran.r-project.org/). Continuous variables (expressed as mean ± standard deviation upon confirmation of normality by Shapiro-Wilk test) and categorical variables (reported as frequencies with proportions) were compared through multivariable regression models adjusted for demographic/clinical confounders; statistical significance was defined as bidirectional P<0.05 with Benjamini-Hochberg correction for multiple comparisons. Survival endpoints were evaluated via stratified log-rank tests and hazard ratios (95% confidence intervals). Data from CCK-8, TUNEL and western blots were treated as continuous variables. Differences between two experimental groups were assessed exclusively by unpaired two-tailed Student's t-tests. Differences between multiple experimental groups and a single control group were assessed using one-way ANOVA followed by Dunnett's multiple comparisons test. To evaluate the monotonic relationship between risk score and dendritic cells activated score, Spearman's rank-order correlation analysis was employed. This non-parametric method was selected since the data were either ordinal or continuous but failed to meet the assumption of normality, as assessed by the Shapiro-Wilk test. P<0.05 was considered to indicate a statistically significant difference.

Results

STING as an adverse prognostic factor in PAAD. To elucidate the clinical significance of the STING pathway in PAAD, its expression profile and prognostic relevance were systematically analyzed. Analysis of the Curated Cancer Cell Atlas revealed predominant STING expression within tumor cells, macrophages, T cells and endothelial cells of the PAAD TME (Fig. 1A) (The Cancer Genome Atlas PAAD cohort; https://portal.gdc.cancer.gov/projects/TCGA-PAAD). Utilizing GEPIA2, significantly elevated STING expression was identified in PAAD compared with normal tissue (Fig. 1B), which was associated with a poor patient prognosis (Fig. 1C) and with progressively with advancing clinical stage (22) (Fig. 1D). Genomic analysis demonstrated that STING alterations in PAAD primarily involved gene amplification (Fig. 1E). Immunohistochemical validation via The Human Protein Atlas database (https://www.proteinatlas.org) confirmed stronger STING protein staining in PAAD tissues compared with that in normal pancreatic ductal epithelium, with STING predominantly localized within cancer nests (Fig. 1F) Collectively, these findings established STING as an adverse prognostic factor in PAAD.

Molecular subtyping of PAAD based on STING pathway genes. Given the prognostic relevance of STING, its core signaling network was characterized to define molecular subtypes. Protein-protein interaction analysis (performed using STRING database v12.0; cn.string-db.org) identified 26 STING signaling pathway-associated genes (Pearson r>0.6; all correlations significant at P<0.001 after Benjamini-Hochberg correction) (Fig. 2A and B). Unsupervised clustering based on the expression profiles of these genes stratified patients with PAAD (TCGA cohort) into two distinct molecular subtypes: Cluster 1 (C1, STING-high) and Cluster 2 (C2, STING-low) (Fig. 2C). Genes within the STING pathway were significantly upregulated in the C1 subtype (Fig. 2D). Survival analysis confirmed that patients with the C1 subtype exhibited significantly worse overall survival (Fig. 2E).

Genomic and immune landscape of STING-defined subtypes. Differential gene expression analysis between C1 and C2 subtypes revealed distinct transcriptional profiles (Fig. 3A and B). Gene Ontology (GO) enrichment analysis of differentially expressed genes highlighted associations with 'adaptive immune response', 'immunoglobulin complex' and 'production of molecular mediator of immune response' (Fig. 3C). Kyoto Encyclopedia of Genes and genomes (KEGG) pathway analysis implicated 'cytokine-cytokine receptor interaction', 'hematopoietic cell lineage' and 'primary immunodeficiency' (Fig. 3D). Mutation profiling demonstrated significantly higher tumor mutational burden in the C1 subtype compared with that in the C2 subtype, characterized by frequent mutations in key oncogenes (GTPase KRas, TP53-binding protein 1, mothers against decapentaplegic homolog 4, tumor suppressor ARF and titin) (Fig. 3E and F). Evaluation of TME composition using ESTIMATE revealed significantly higher immune and stromal scores and lower tumor purity in C1 vs. C2 (Fig. 4A-D). CIBERSORTx deconvolution further indicated elevated infiltration of T cells γ δ in the C1 subtype (Fig. 4E). Consistent with enhanced immunogenicity, C1 exhibited significantly higher expression of human leukocyte antigen family genes and immune checkpoint molecules relative to C2 (Fig. 4F and G).

Development and validation of a STING pathway prognostic signature. A risk prediction model was constructed to quantify the prognostic heterogeneity associated with STING pathway activity. Univariate Cox regression analysis identified 10 genes among the 26 STING pathway genes that were significantly associated with PAAD prognosis (Fig. 5A). LASSO Cox regression refined these into a 6-gene prognostic signature [deltex E3 ubiquitin ligase 4, interferon γ inducible protein 16, mitochondrial antiviral-signaling protein (MAVS), protein kinase DNA-activated catalytic subunit, ZDHHC1 and IFIT2] (Fig. 5B and C). This signature effectively stratified patients with PAAD into high- and low-risk groups. Survival outcomes were significantly different in the TCGA discovery cohort (Fig. 5D) and the independent GSE224564 validation cohort (Fig. 5E). Expression patterns of the 6 signature genes were consistent across both TCGA (Fig. 5F) and validation cohort (Fig. 5G) datasets. Notably, multivariate Cox regression analysis confirmed both the prognostic risk score and N stage as independent predictors of survival in patients with PAAD (Fig. 6A and B).

Association of prognostic risk score with immune features. The STING pathway-derived prognostic risk score demonstrated

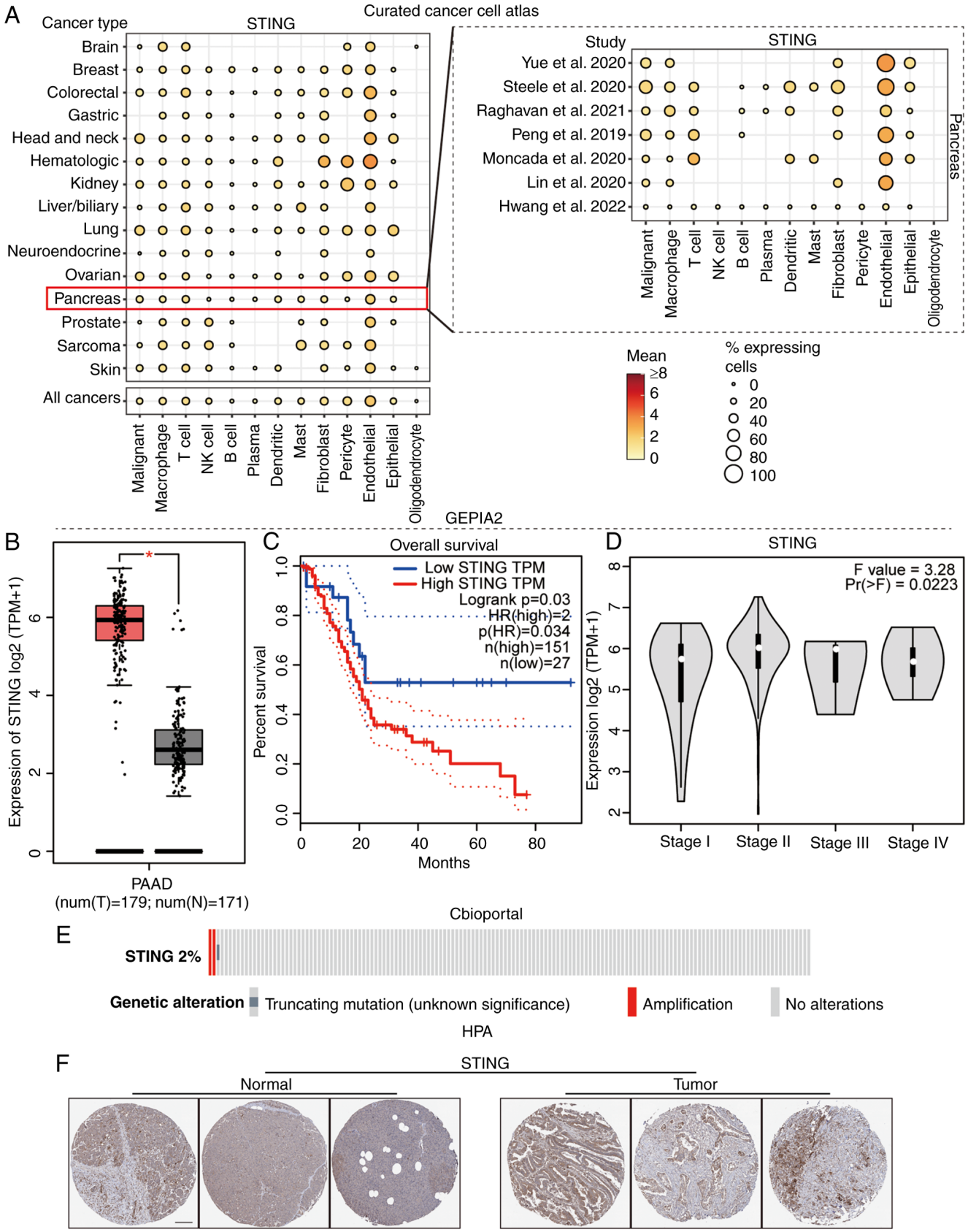


Figure 1. Role of STING expression in PAAD. (A) Heatmap comparing STING and immune-related gene expression profiles in PAAD tumor microenvironment vs. adjacent normal tissue. (B) Box plot demonstrating significantly elevated STING mRNA expression in PAAD tumors (T) vs. normal pancreatic tissues (N) (*P<0.05) (TCGA-PAAD (T) + Genotype-Tissue Expression; normal controls; https://gtexportal.org). (C) Kaplan-Meier curves comparing overall survival between PAAD patients with low vs. high STING expression (log-rank test). (D) Violin plots showing STING expression distribution across AJCC stages (I-IV) of PAAD. (E) Oncoprint of STING genomic alterations (mutations, copy number changes) in PAAD. (F) Human Protein Atlas representative immunohistochemistry images of STING protein expression (PAAD tissue; proteinatlas.org). Scale bar, 100 μm. STING, stimulator of interferon genes; PAAD, pancreatic ductal adenocarcinoma; PAAD, pancreatic adenocarcinoma; IHC, immunohistochemistry; NK, natural killer; HR, hazard ratio; T, tumor; N, normal; TPM, transcripts per million.

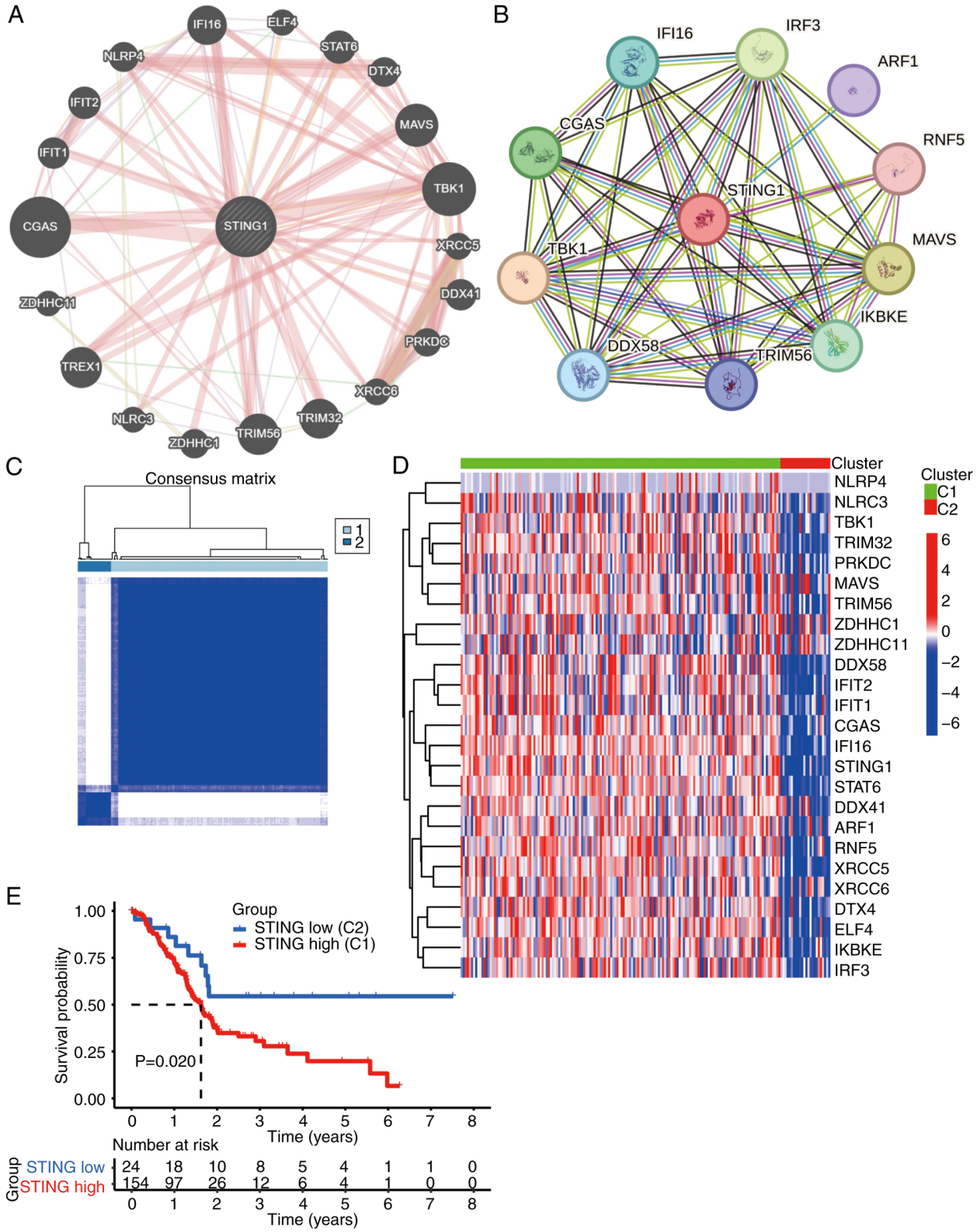


Figure 2. Molecular characterization of STING signaling pathway-related genes in PAAD. (A) Protein-protein interaction (PPI) network of core STING signaling components identified through STRING database analysis (minimum interaction score: 0.4). (B) Expanded PPI network showing secondary interactors of STING pathway genes (minimum interaction score: 0.7). (C) Consensus matrix heatmap classifying patients with PAAD into two molecular subtypes (C1 and C2) based on STING-related gene expression patterns. (D) Heatmap comparing expression profiles of STING-related genes across PAAD subtypes (C1 vs. C2) with expression gradient key (red, high expression; blue, low expression). (E) Kaplan-Meier survival analysis showing significantly reduced overall survival in the STING-enriched subtype (C1) compared with the STING-depleted subtype (C2). STING, stimulator of interferon genes; PAAD, pancreatic ductal adenocarcinoma; CGAS, cyclic GMP-AMP synthase; TBK1, TANK-binding kinase 1; MAVS, mitochondrial antiviral-signaling protein; TRIM56, tripartite motif-containing 56; TREX1, three prime repair exonuclease 1; TRIM32, tripartite motif-containing 32; IFI16, interferon γ inducible protein 16; IFIT1, interferon-induced protein with tetratricopeptide repeats 1; DDX41, DEAD-box helicase 41; NLRP4, NLR family pyrin domain containing 4; DTX4, deltex E3 ubiquitin ligase 4; ZDHHC1, zinc finger DHHC-type containing 1; PRKDC, protein kinase DNA-activated catalytic subunit; XRCC, X-ray repair cross complementing; ELF4, E74-like ETS transcription factor 4; NLRC3, NLR family CARD domain containing 3; ARF1, ARF GTPase 1; DDX56, RNA sensor RIG-I; IKBKE, inhibitor of nuclear factor κB kinase subunit ε; IRF3, interferon regulatory factor 3; RNF5, ring finger protein 5.

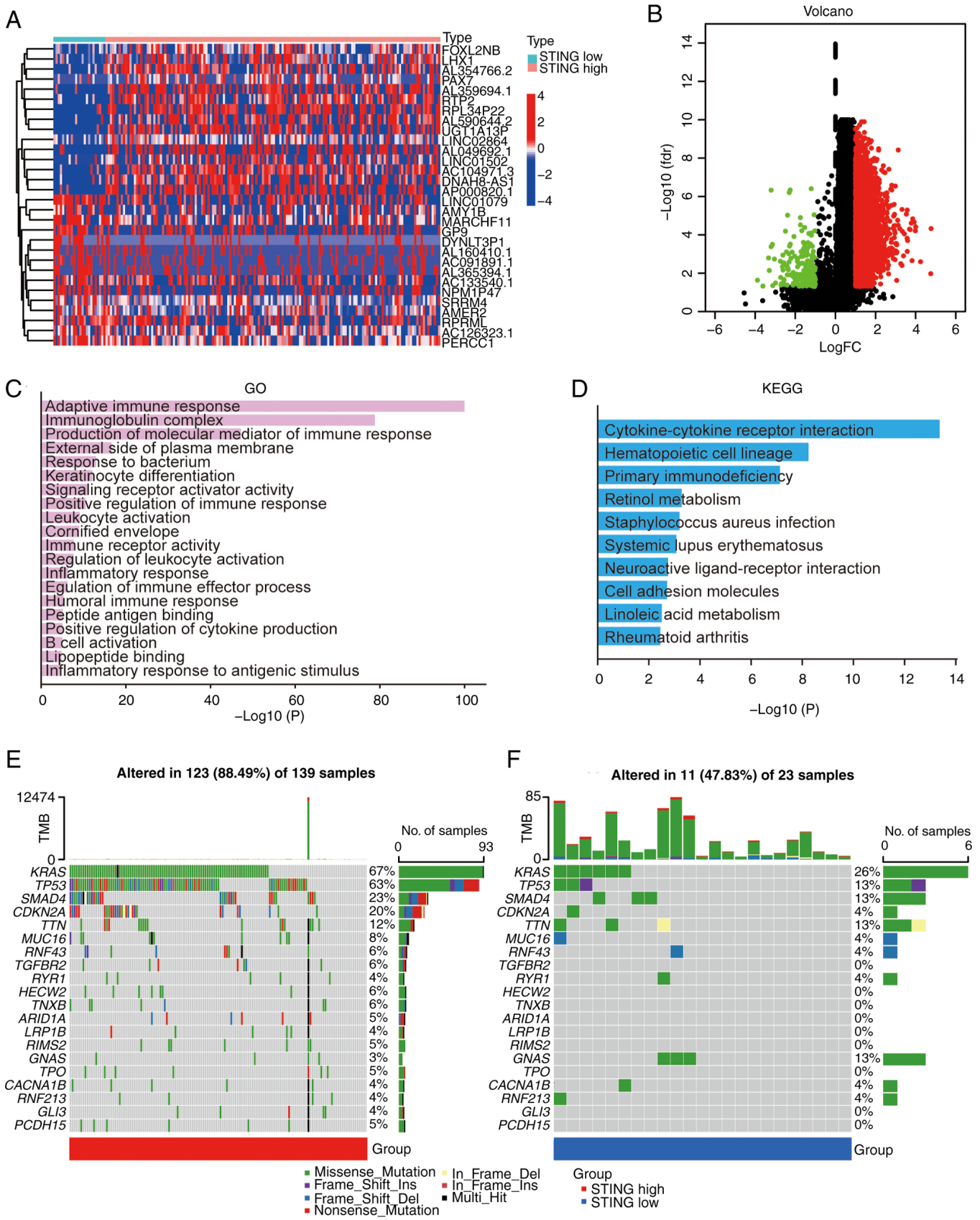


Figure 3. Gene characteristics of different PAAD subtypes. (A) Heatmap of upregulated genes in STING1-enriched subtype (C1) vs. STING1-depleted subtype (C2). (B) Heatmap of downregulated genes in STING1-enriched subtype (C1) vs. STING1-depleted subtype (C2). (red, high expression; blue, low expression). (C) GO enrichment analysis showing top biological processes in STING1-enriched subtype. (D) KEGG pathway enrichment analysis showing top signaling pathways in STING1-enriched subtype. (E) Mutational landscape of STING1-enriched subtype (C1) showing frequent mutations in KRAS, TP53 and CDKN2A. (F) Mutational landscape of STING1-depleted subtype (C2) showing distinct mutation profile with SMAD4 alterations. PAAD, pancreatic ductal adenocarcinoma; STING, stimulator of interferon genes; FC, fold-change; fdr, false discovery rate; TMB, tumor mutational burden; GO, Gene Ontology; KEGG, Kyoto Encyclopedia of Genes and Genomes.

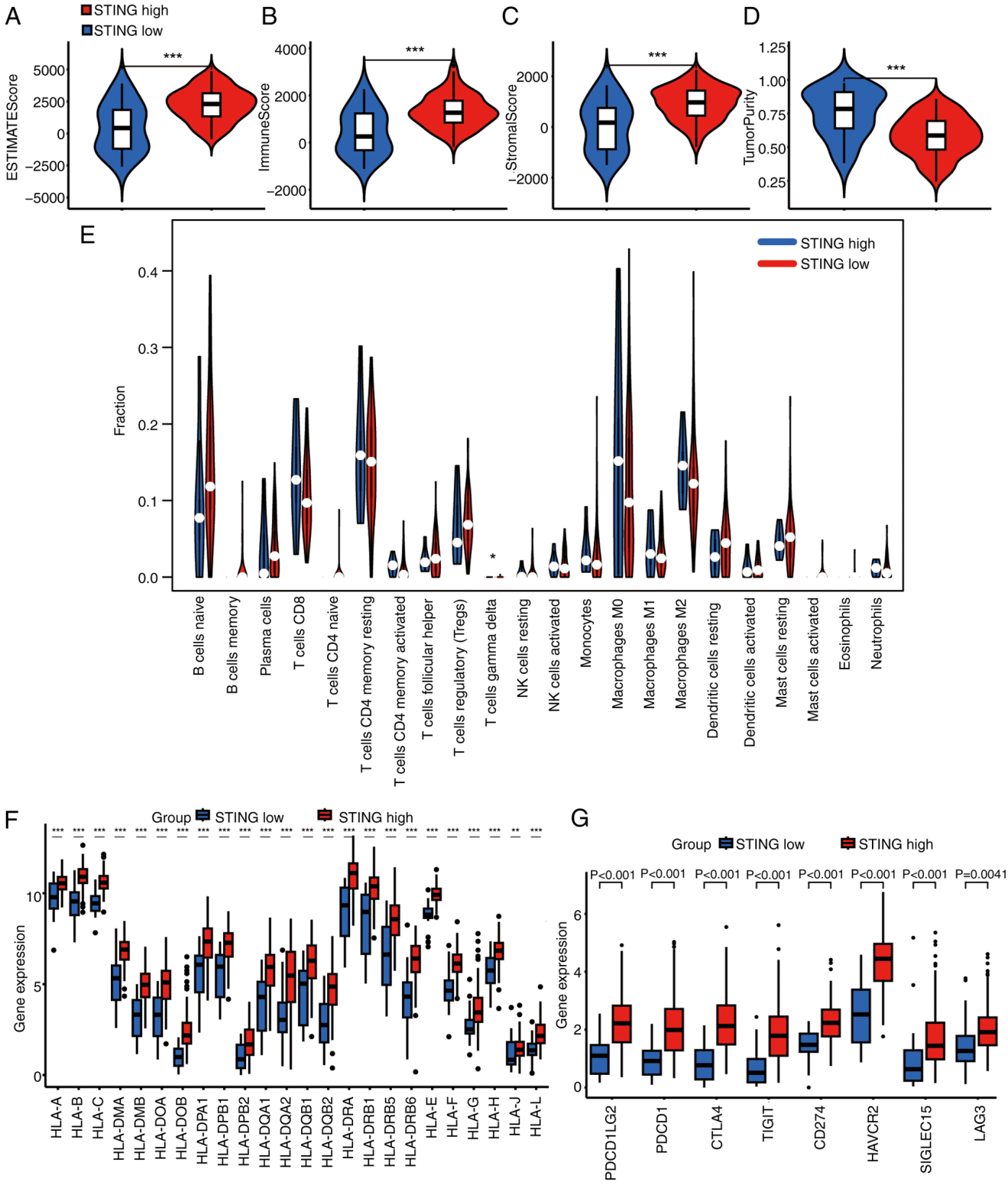


Figure 4. Immune microenvironment profiling of PAAD molecular subtypes. (A) ESTIMATE analysis showing significantly higher immune scores in STING1-high subtype (C1) vs. STING1-low subtype (C2). (B) Significantly higher stromal scores in C1 vs. C2. (C) Significantly lower tumor purity in C1 vs. C2. (D) CIBERSORT analysis revealing differential immune cell infiltration patterns between subtypes (key immune subsets labeled) (***P<0.001). (E) Positive correlation between STING1 expression and γδ T cell infiltration density (Pearson r=0.68; *P<0.05) (F) Upregulated HLA molecule expression in C1 vs. C2 (**P<0.05 and ***P<0.01). (G) Elevated immune checkpoint molecule expression in C1 vs. C2. PAAD, pancreatic ductal adenocarcinoma; STING, stimulator of interferon genes; HLA, human leukocyte antigen; NK, natural killer.

significant biological relevance, showing a positive correlation with DC activation as determined by Spearman's rank correlation analysis (Fig. 6C). Assessment using the TIDE algorithm revealed significantly higher scores in high-risk vs. low-risk patients, indicating greater immune evasion potential and reduced likelihood of response to immune

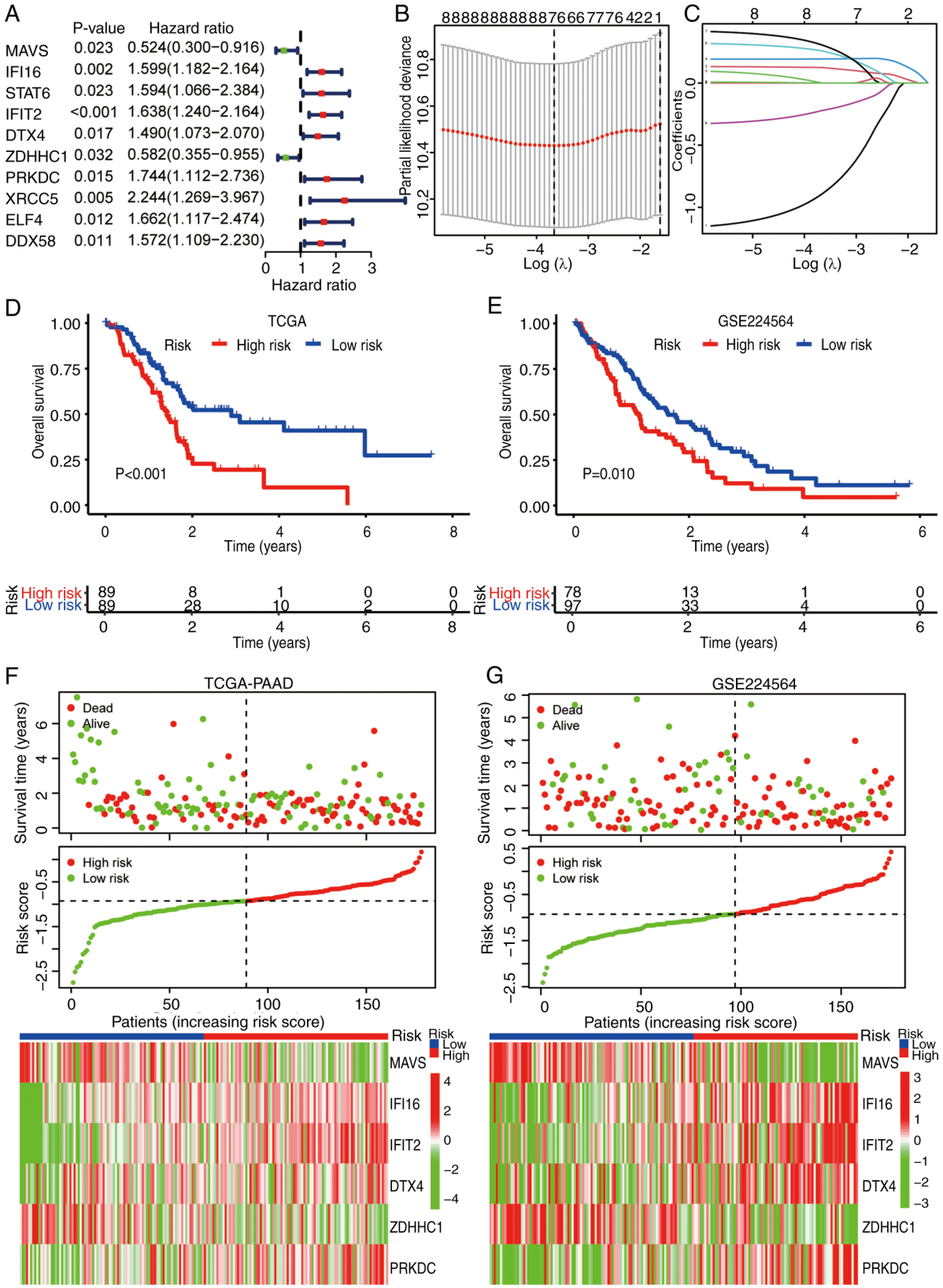


Figure 5. Development and validation of a STING1 signaling-related prognostic signature for PAAD. (A) Univariate Cox regression analysis of STING1 pathway-related genes in PAAD. Genes with significant prognostic value (P<0.05) are included. (B) LASSO regression 10-fold cross-validation curve showing optimal λ selection (minimum criteria). (C) LASSO coefficient profiles of STING1-related genes across log(λ) sequence. (D) Kaplan-Meier survival analysis for the prognostic signature in TCGA-PAAD cohort (high-risk vs. low-risk groups; cutoff: median risk score). (E) Validation of prognostic signature in GSE224564 cohort. (F) Risk score distribution plot with corresponding survival status and expression heatmap for 6 signature genes in TCGA-PAAD. (G) Validation in GSE224564 cohort showing identical configuration to (F). STING, stimulator of interferon genes; PAAD, pancreatic ductal adenocarcinoma; LASSO, least absolute shrinkage and selection operator; TCGA, The Cancer Genome Atlas; MAVS, mitochondrial antiviral-signaling protein; IFI16, interferon γ inducible protein 16; IFIT2, interferon-induced protein with tetratricopeptide repeats 2; DTX4, deltex E3 ubiquitin ligase 4; ZDHHC1, zinc finger DHHC-type containing 1; PRKDC, protein kinase DNA-activated catalytic subunit; STAT6, signal transducer and activator of transcription 6; XRCC5, X-ray repair cross complementing: ELF4, E74-like ETS transcription factor 4; DDX58, RNA sensor RIG-I.

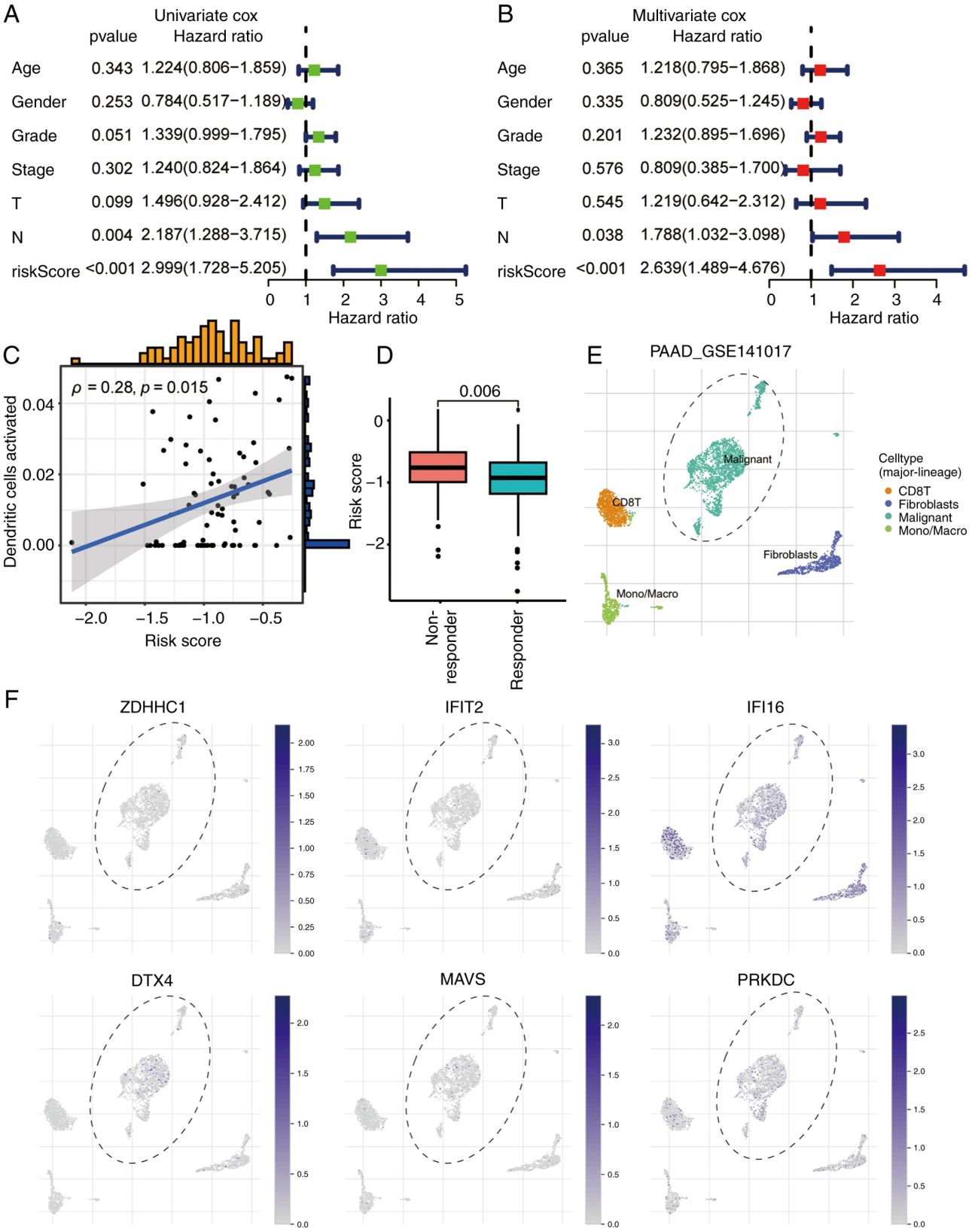


Figure 6. Independent prognostic value and immunotherapy relevance of the STING-related risk signature in PAAD. (A) Univariate Cox regression analysis of clinical parameters and risk score. (B) Multivariate Cox regression confirming the risk score as an independent prognostic factor after adjusting for covariates in (A). (C) Correlation analysis of risk score and activated dendritic cell abundance. 'Dendritic cells activated' represents proportion scores derived from the xCell algorithm (0-1 scale), quantifying relative abundance in the tumor microenvironment. Correlation was assessed using Spearman's rank correlation analysis (Spearman's ρ=0.28; P=0.015). (D) Higher risk scores in immunotherapy non-responders vs. responders (Mann-Whitney U test). Single-cell RNA sequencing (GSE141017) visualization of STING1 signature gene expression: (E) t-SNE plot showing cell-type distribution. (F) Feature plots of signature gene expression across the PAAD tumor microenvironment. STING, stimulator of interferon genes; PAAD, pancreatic ductal adenocarcinoma; T, tumor; N, node; CD8T, T-cell surface glycoprotein CD8; ZDHHC1, zinc finger DHHC-type containing 1; IFIT2, interferon-induced protein with tetratricopeptide repeats 2; IFI16, interferon γ inducible protein 16; DTX4, deltex E3 ubiquitin ligase 4; MAVS, mitochondrial antiviral-signaling protein; PRKDC, protein kinase DNA-activated catalytic subunit; PAAD, pancreatic adenocarcinoma.

checkpoint blockade (Fig. 6D). Analysis of spatial expression (GSE141017) confirmed that the 6 signature genes were predominantly expressed within tumor cells of the PAAD TME (Fig. 6E and F).

Functional validation of hub genes IFIT2 and ZDHHC1. Given the established prognostic relevance of STING in PAAD (characterized by high expression correlating with poor patient outcomes in the present study), its core signaling network was characterized to define molecular subtypes. While MAVS demonstrated strong prognostic associations, its functional role in PAAD has been extensively explored in prior literature (23). By contrast, ZDHHC1 and IFIT2, which also showed significant prognostic value (Fig. S1), have received considerably less attention in PAAD research. These genes were therefore prioritized for validation, observing distinct expression dynamics: IFIT2 expression significantly increased with advancing AJCC 8th edition tumor grade/stage (22) up to stage III/grade 3 before declining in advanced disease, associated with a poor prognosis, while ZDHHC1 expression decreased progressively with tumor progression and was associated with favorable outcomes (Fig. S1A-E). Immunohistochemical validation using The Human Protein Atlas (https://www.proteinatlas.org) confirmed these protein patterns in PAAD tissues (Fig. 7A). Overexpression of ZDHHC1 was confirmed in the Panc-02 cells line (Fig. 7B). Based on the confirmed superior knockdown efficiency of sh2, the stable cell line expressing sh2 was selected for all subsequent functional experiments (Fig. 7C). Functional studies in Panc02 cells revealed that overexpression of ZDHHC1 inhibited proliferation (Fig. 7D), as did knockdown of IFIT2 (Fig. 7E). Overexpression of ZDHHC1 (Fig. 7F) and knockdown of IFIT2 (Fig. 7G) both promoted apoptosis. These results established IFIT2 as a potential oncogene and ZDHHC1 as a potential tumor suppressor within the STING pathway in PAAD.

Discussion

PAAD presents a notable global health challenge, ranking 12th in global cancer incidence but 7th in cancer-related mortality rate according to 2020 data (24), with similar trends observed in China (25). Bioinformatics has emerged as a powerful tool for dissecting PAAD pathogenesis (26), enabling the identification of potential biomarkers, therapeutic targets and immune evasion mechanisms through the integrated analysis of genomic, transcriptomic and tumor microenvironmental data (27).

Research into the STING signaling pathway in PAAD reveals its complex duality. While STING agonists activate the cyclic GMP-AMP synthase-STING pathway to induce IFN-I, trigger adaptive immunity and exert cytotoxic effects on tumor cells (11), clinical translation has been hampered by intrinsic resistance mechanisms (28). These include STING-induced expansion of regulatory B cells that suppress natural killer cell activity (29) and the potential for chronic pathway activation to promote immunosuppressive signaling downstream of chromosomal instability (30). Nevertheless, STING agonism demonstrates significant preclinical promise as it remodels the PAAD tumor stroma and immune landscape, enhances cytotoxic T cell infiltration while reducing the frequency of regulatory T cells (31), activates DCs and reprograms macrophages towards an immunostimulatory phenotype (32). Furthermore, synergistic strategies, such as combining STING agonists with interleukin-35 blockade, show enhanced antitumor efficacy (29). Future progress may hinge on developing novel agonists (for example, non-nucleotide compounds) and targeted delivery systems to improve efficacy and minimize toxicity.

The present study provides novel insights into the immune-related functions of STING and its associated genes within the distinct context of PAAD. Notably, high expression of STING pathway genes was identified to be associated with a poor prognosis in PAAD. This association contrasts with observations in some other cancer types (such as gastric cancer, colorectal cancer and hepatocellular carcinoma) and potentially reflects the unique immunobiology of the 'cold' nature of PAAD tumors. Using this, a robust prognostic signature centered on STING pathway activity was developed. Further functional prioritization within this signature highlighted the notable, yet opposing, roles of IFIT2 and ZDHHC1.

In the present study, IFIT2 emerged as a potential oncogenic driver in PAAD. Elevated IFIT2 expression was associated with advanced tumor grade/stage (22) and worse survival outcomes. This association aligns with studies linking IFIT2 to chemotherapy resistance in PAAD and its established role in regulating inflammatory responses downstream of IFN signaling and pathogen recognition (33). IFIT2 may modulate the tumor immune microenvironment (TIME); evidence in esophageal squamous cell carcinoma shows that methyltransferase-like protein 3-mediated neuronal membrane glycoprotein M6-a modification regulates IFIT2, influencing malignant progression and the TIME (34). While prognostic in oral squamous cell carcinoma, the specific pro-tumorigenic mechanisms of IFIT2 in PAAD warrant further investigation. Conversely, in the present study, ZDHHC1 functioned as a putative tumor suppressor. ZDHHC1 is frequently epigenetically silenced via promoter methylation across various cancer types, such as gastric cancer, colorectal cancer and hepatocellular carcinoma. Restoring ZDHHC1 expression exerts broad antitumor effects, including the induction of apoptosis and autophagy, cell cycle arrest, the inhibition of migration/metastasis, the reversal of epithelial-mesenchymal transition and stemness (35), and metabolic reprogramming via suppression of glycolysis and the pentose phosphate pathway (36). Mechanistically, ZDHHC1 acts as an S-palmitoyltransferase critical for palmitoylating p53 at residues C135, C176 and C275, thereby stabilizing and activating the master tumor suppressor activity of p53 (37). Loss of ZDHHC1-mediated p53 palmitoylation represents a novel evasion mechanism in cancer. Although the role of ZDHHC1 in PAAD was previously undefined, the present data positions ZDHHC1 as a compelling therapeutic target meriting further exploration in PAAD.

While providing valuable mechanistic and prognostic insights into STING signaling in PAAD, the present study has several limitations: i) The reliance on protein-protein interaction networks for gene selection may have excluded key epigenomic regulators or microenvironmental modulators, limiting pathway comprehensiveness; ii) despite

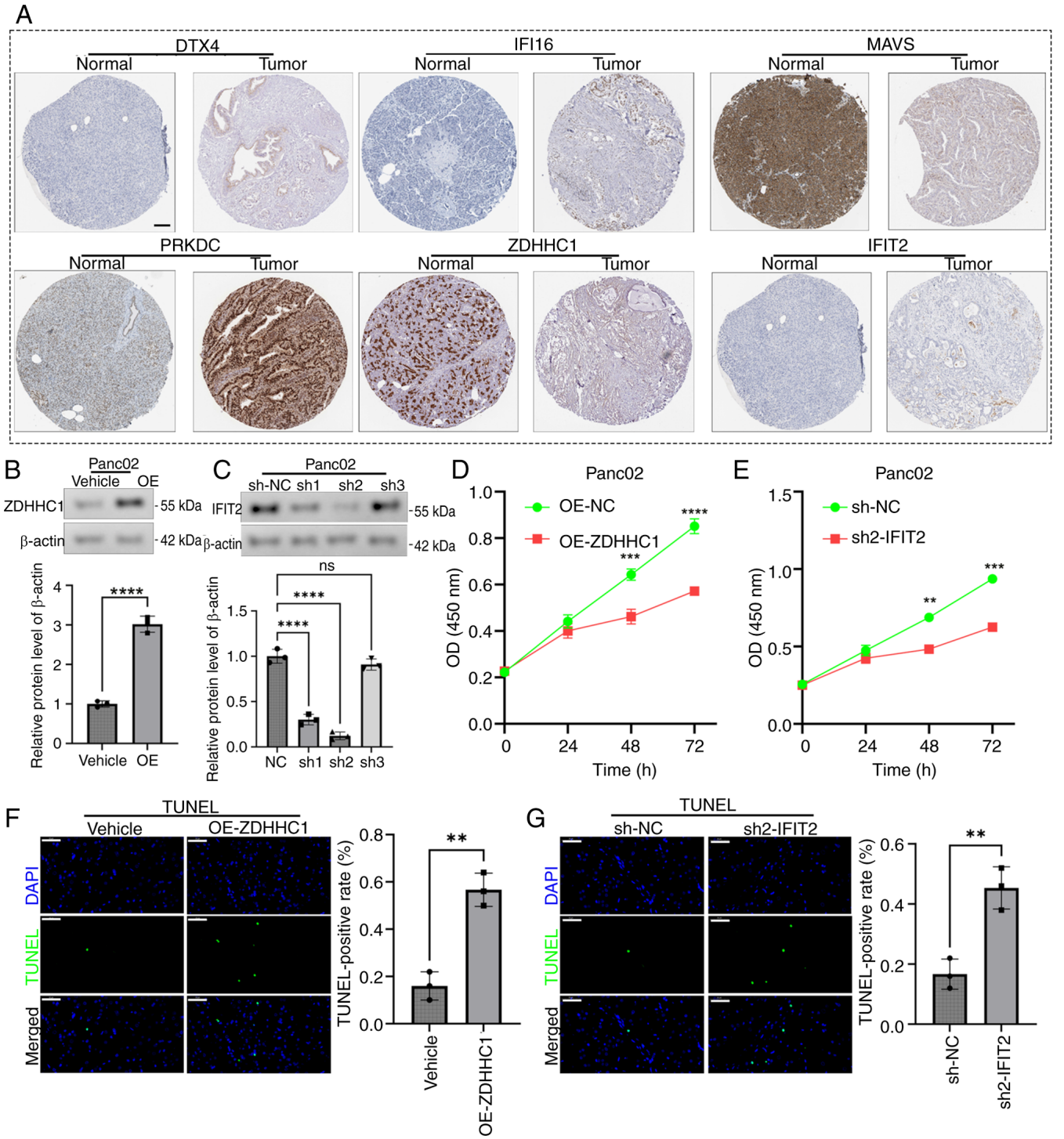


Figure 7. Functional roles of IFIT2 and ZDHHC1 in PAAD oncobiology. (A) Human Protein Atlas representative immunohistochemical staining of six prognostic signature genes in PAAD tissues (proteinatlas.org). Scale bar, 100 μm. (B) Western blot and semi-quantification confirming successful ZDHHC1 overexpression in Panc02 cells (C) Western blot and semi-quantification confirming IFIT2 knockout efficiency in Panc02 cells (****P<0.0001). (D) CCK-8 assay: ZDHHC1 overexpression enhances Panc02 proliferation (***P<0.001 and ****P<0.0001 vs OE-NC). (E) CCK-8 assay: IFIT2 knockout enhances Panc02 proliferation (**P<0.01 and ***P<0.001 vs. sh-NC). (F) TUNEL assay (scale bar, 50 μm) demonstrating reduced apoptosis in ZDHHC1-overexpressing Panc02 cells. (G) TUNEL assay (scale bar 50 μm) showing decreased apoptosis in IFIT2-knockout Panc02 cells (**P<0.01). IFIT2, interferon-induced protein with tetratricopeptide repeats 2; ZDHHC1, zinc finger DHHC-type containing 1; PAAD, pancreatic ductal adenocarcinoma; OE, overexpression; CCK-8, Cell Counting Kit-8; DTX4, deltex E3 ubiquitin ligase 4; IFI16, interferon γ inducible protein 16; MAVS, mitochondrial antiviral-signaling protein; PRKDC, protein kinase DNA-activated catalytic subunit; sh-NC, scrambled negative control shRNA; ns, not significant.

internal-external validation (TCGA + GSE224564, n=353), cohort size constraints limit statistical power for detailed subtype-specific analyses and robust assessment of treatment interactions; iii) while *in vitro* validation confirmed IFIT2/ZDHHC1 functionality in Panc02 cells, the present study lacked *in vivo* models to evaluate stromal cross-talk, combinatorial gene perturbation assays to assess IFIT2-ZDHHC1 interplay and spatial resolution of immune

effects (for example, multiplexed T-cell infiltration mapping); iv) clinical translation requires standardized detection protocols for biopsy specimens and prospective trials stratifying immunotherapy based on risk scores; and v) the cellular origin (cancer vs. immune) and temporal dynamics of STING pathway gene expression during progression remain unresolved. Future research should prioritize multi-center signature validation, developing CRISPR-engineered dual-gene models (IFIT2 knockout + ZDHHC1 overexpression) for *in vivo* efficacy testing, employing spatial multi-omics (single cell RNA sequencing and spatial proteomics) to resolve compartment-specific expression and conducting STING agonist trials within signature-defined patient subgroups.

In summary, the present study established and validated a STING signaling pathway-derived prognostic gene signature that effectively stratifies patients with PAAD. High-risk patients identified by this signature exhibited significantly poorer survival outcomes compared with low-risk patients, and distinct immune microenvironment profiles. Notably, the antagonistic roles of two core signature genes were functionally validated: IFIT2 as a potential oncogene promoting proliferation and suppressing apoptosis, and ZDHHC1 as a putative tumor suppressor with the converse effects. The findings of the present study underscore the notable clinical and biological relevance of the STING pathway in PAAD. The identified genes, particularly IFIT2 and ZDHHC1, represent promising candidates for further mechanistic exploration and potential targets for developing novel therapeutic strategies against this lethal malignancy.

Acknowledgements

Not applicable.

Funding

No funding was received.

Availability of data and materials

The data generated in the present study may be requested from the corresponding author.

Authors' contributions

WY and JLia contributed to the conceptualization, reviewing and editing of the manuscript. JLi was responsible for the curation of the data. YW provided the formal analysis and supervision. All authors read and approved the final version of the manuscript. JLi and YW confirm the authenticity of all the raw data.

Ethics approval and consent to participate

Not applicable.

Patient consent for publication

Not applicable.

Competing interests

The authors declare that they have no competing interests.

References

1. Bray F, Laversanne M, Sung H, Ferlay J, Siegel RL, Soerjomataram I and Jemal A: Global cancer statistics 2022: GLOBOCAN estimates of incidence and mortality worldwide for 36 cancers in 185 countries. CA Cancer J Clin 74: 229-263, 2024.
2. Blackford AL, Canto MI, Dbouk M, Hruban RH, Katona BW, Chak A, Brand RE, Syngal S, Farrell J, Kastrinos F, *et al*: Pancreatic cancer surveillance and survival of high-risk individuals. JAMA Oncol 10: 1087-1096, 2024.
3. Park W, Chawla A and O'Reilly EM: Pancreatic cancer: A review. JAMA 326: 851-862, 2021.
4. Peduzzi G, Archibugi L, Farinella R, de Leon Pisani RP, Vodickova L, Vodicka P, Kraja B, Sainz J, Bars-Cortina D, Daniel N, *et al*: The exposome and pancreatic cancer, lifestyle and environmental risk factors for PDAC. Semin Cancer Biol 113: 100-129, 2025.
5. Springfeld C, Ferrone CR, Katz MHG, Philip PA, Hong TS, Hackert T, Büchler MW and Neoptolemos J: Neoadjuvant therapy for pancreatic cancer. Nat Rev Clin Oncol 20: 318-337, 2023.
6. Hu ZI and O'Reilly EM: Therapeutic developments in pancreatic cancer. Nat Rev Gastroenterol Hepatol 21: 7-24, 2024.
7. Sang W, Zhou Y, Chen H, Yu C, Dai L, Liu Z, Chen L, Fang Y, Ma P, Wu X, *et al*: Receptor-interacting protein kinase 2 is an immunotherapy target in pancreatic cancer. Cancer Discov 14: 326-347, 2024.
8. Ullman NA, Burchard PR, Dunne RF and Linehan DC: Immunologic strategies in pancreatic cancer: Making cold tumors hot. J Clin Oncol 40: 2789-2805, 2022.
9. Zhao K, Huang J, Zhao Y, Wang S, Xu J and Yin K: Targeting STING in cancer: Challenges and emerging opportunities. Biochim Biophys Acta Rev Cancer 1878: 188983, 2023.
10. Zhang B, Xu P and Ablasser A: Regulation of the cGAS-STING pathway. Annu Rev Immunol 43: 667-692, 2025.
11. Tani T, Mathsyaraja H, Campisi M, Li ZH, Haratani K, Fahey CG, Ota K, Mahadevan NR, Shi Y, Saito S, *et al*: TREX1 inactivation unleashes cancer cell STING-interferon signaling and promotes antitumor immunity. Cancer Discov 14: 752-765, 2024.
12. Luo J, Wang S, Yang Q, Fu Q, Zhu C, Li T, Yang S, Zhao Y, Guo R, Ben X, *et al*: γδ T Cell-mediated tumor immunity is tightly regulated by STING and TGF-β signaling pathways. Adv Sci (Weinh) 12: e2404432, 2025.
13. Liu X, Hogg GD, Zuo C, Borcherding NC, Baer JM, Lander VE, Kang LI, Knolhoff BL, Ahmad F, Osterhout RE, *et al*: Context-dependent activation of STING-interferon signaling by CD11b agonists enhances anti-tumor immunity. Cancer Cell 41: 1073-1090.e12, 2023.
14. Tian X, Ai J, Tian X and Wei X: cGAS-STING pathway agonists are promising vaccine adjuvants. Med Res Rev 44: 1768-1799, 2024.
15. Chen X, Xu Z, Li T, Thakur A, Wen Y, Zhang K, Liu Y, Liang Q, Liu W, Qin JJ and Yan Y: Nanomaterial-encapsulated STING agonists for immune modulation in cancer therapy. Biomark Res 12: 2, 2024.
16. Chin EN, Sulpizio A and Lairson LL: Targeting STING to promote antitumor immunity. Trends Cell Biol 33: 189-203, 2023.
17. Chen X, Meng F, Xu Y, Li T, Chen X and Wang H: Chemically programmed STING-activating nano-liposomal vesicles improve anticancer immunity. Nat Commun 14: 4584, 2023.
18. Dosta P, Cryer AM, Dion MZ, Shiraishi T, Langston SP, Lok D, Wang J, Harrison S, Hatten T, Ganno ML, *et al*: Investigation of the enhanced antitumour potency of STING agonist after conjugation to polymer nanoparticles. Nat Nanotechnol 18: 1351-1363, 2023.
19. Wen Z, Sun F, Wang R, Wang W, Zhang H, Yang F, Wang M, Wang Y and Li B: STING agonists: A range of eminent mediators in cancer immunotherapy. Cell Signal 134: 111914, 2025.
20. Ohara Y, Tang W, Liu H, Yang S, Dorsey TH, Cawley H, Moreno P, Chari R, Guest MR, Azizian A, *et al*: SERPINB3-MYC axis induces the basal-like/squamous subtype and enhances disease progression in pancreatic cancer. Cell Rep 42: 113434, 2023.
21. Amin MB, Greene FL, Edge SB, Compton CC, Gershenwald JE, Brookland RK, Meyer L, Gress DM, Byrd DR and Winchester DP: The eighth edition AJCC cancer staging manual: Continuing to build a bridge from a population-based to a more 'personalized' approach to cancer staging. CA Cancer J Clin 67: 93-99, 2017.

22. Lee M, Thomas AS, Lee SY, Cho YJ, Jung HS, Yun WG, Han Y, Jang JY, Kluger MD and Kwon W: Reconsidering the absence of extrapancreatic extension in T staging for pancreatic adenocarcinoma in the AJCC (8th ed) staging manual using the national cancer database. J Gastrointest Surg 27: 2484-2492, 2023.
23. Kerschbaum-Gruber S, Kleinwächter A, Popova K, Kneringer A, Appel LM, Stasny K, Röhrer A, Dias AB, Benedum J, Walch L, *et al*: Cytosolic nucleic acid sensors and interferon beta-1 activation drive radiation-induced anti-tumour immune effects in human pancreatic cancer cells. Front Immunol 15: 1286942, 2024.
24. Sung H, Ferlay J, Siegel RL, Laversanne M, Soerjomataram I, Jemal A and Bray F: Global cancer statistics 2020: GLOBOCAN estimates of incidence and mortality worldwide for 36 cancers in 185 countries. CA Cancer J Clin 71: 209-249, 2021.
25. Yin L, Wei J, Lu Z, Huang S, Gao H, Chen J, Guo F, Tu M, Xiao B, Xi C, *et al*: Prevalence of germline sequence variations among patients with pancreatic cancer in China. JAMA Netw Open 5: e2148721, 2022.
26. Larson NB, Oberg AL, Adjei AA and Wang L: A clinician's guide to bioinformatics for next-generation sequencing. J Thorac Oncol 18: 143-157, 2023.
27. Petralia F, Ma W, Yaron TM, Caruso FP, Tignor N, Wang JM, Charytonowicz D, Johnson JL, Huntsman EM, Marino GB, *et al*: Pan-cancer proteogenomics characterization of tumor immunity. Cell 187: 1255-1277.e27, 2024.
28. Lv M, Chen M, Zhang R, Zhang W, Wang C, Zhang Y, Wei X, Guan Y, Liu J, Feng K, *et al*: Manganese is critical for antitumor immune responses via cGAS-STING and improves the efficacy of clinical immunotherapy. Cell Res 30: 966-979, 2020.
29. Li S, Mirlekar B, Johnson BM, Brickey WJ, Wrobel JA, Yang N, Song D, Entwistle S, Tan X, Deng M, *et al*: STING-induced regulatory B cells compromise NK function in cancer immunity. Nature 610: 373-380, 2022.
30. Li J, Hubisz MJ, Earlie EM, Duran MA, Hong C, Varela AA, Lettera E, Deyell M, Tavora B, Havel JJ, *et al*: Non-cell-autonomous cancer progression from chromosomal instability. Nature 620: 1080-1088, 2023.
31. Jneid B, Bochnakian A, Hoffmann C, Delisle F, Djacoto E, Sirven P, Denizeau J, Sedlik C, Gerber-Ferder Y, Fiore F, *et al*: Selective STING stimulation in dendritic cells primes antitumor T cell responses. Sci Immunol 8: eabn6612, 2023.
32. Wang J, Li S, Wang M, Wang X, Chen S, Sun Z, Ren X, Huang G, Sumer BD, Yan N, *et al*: STING licensing of type I dendritic cells potentiates antitumor immunity. Sci Immunol 9: eadj3945, 2024.
33. Yang Y, Song J, Zhao H, Zhang H and Guo M: Patients with dermatomyositis shared partially similar transcriptome signature with COVID-19 infection. Autoimmunity 56: 2220984, 2023.
34. Xu QC, Tien YC, Shi YH, Chen S, Zhu YQ, Huang XT, Huang CS, Zhao W and Yin XY: METTL3 promotes intrahepatic cholangiocarcinoma progression by regulating IFIT2 expression in an m^6A-YTHDF2-dependent manner. Oncogene 41: 1622-1633, 2022.
35. Zhou B, Liu Y, Ma H, Zhang B, Lu B, Li S, Liu T, Qi Y, Wang Y, Zhang M, *et al*: Zdhhc1 deficiency mitigates foam cell formation and atherosclerosis by inhibiting PI3K-Akt-mTOR signaling pathway through facilitating the nuclear translocation of p110α. Biochim Biophys Acta Mol Basis Dis 1871: 167577, 2025.
36. Le X, Mu J, Peng W, Tang J, Xiang Q, Tian S, Feng Y, He S, Qiu Z, Ren G, *et al*: DNA methylation downregulated ZDHHC1 suppresses tumor growth by altering cellular metabolism and inducing oxidative/ER stress-mediated apoptosis and pyroptosis. Theranostics 10: 9495-9511, 2020.
37. Tang J, Peng W, Feng Y, Le X, Wang K, Xiang Q, Li L, Wang Y, Xu C, Mu J, *et al*: Cancer cells escape p53's tumor suppression through ablation of ZDHHC1-mediated p53 palmitoylation. Oncogene 40: 5416-5426, 2021.



Copyright © 2025 Yu et al. This work is licensed under a Creative Commons Attribution-NonCommercial-NoDerivatives 4.0 International (CC BY-NC-ND 4.0) License.